



Synthesis and in vitro study of nitro- and methoxy-2-phenylbenzofurans as human monoamine oxidase inhibitors

Giovanna L. Delogu^{a,1,*}, Amit Kumar^{b,1}, Gianluca Gatto^b, Fernando Bustelo^{c,d},
Lucía M. Saavedra^e, Maria Isabel Rodríguez-Franco^e, Reyes Laguna^c, Dolores Viña^{c,d,*}

^a Department of Life and Environmental Sciences, University of Cagliari, 09042 Monserrato, Cagliari, Italy

^b Department of Electrical and Electronic Engineering, University of Cagliari 09123 Cagliari, Italy

^c Center for Research in Molecular Medicine and Chronic Diseases (CIMUS), University of Santiago de Compostela, Avda Barcelona s/n, Campus Vida 15782, Santiago de Compostela, Spain

^d Department of Pharmacology, Pharmacy and Pharmaceutical Technology, Faculty of Pharmacy, University of Santiago de Compostela, 15782 Santiago de Compostela, Spain

^e Instituto de Química Médica, Consejo Superior de Investigaciones Científicas (IQM-CSIC), c/ Juan de la Cierva 3, E-28006 Madrid, Spain

ARTICLE INFO

Keywords:

2-Phenylbenzofurans
Monoamine oxidase inhibitors
Docking studies

ABSTRACT

A new series of 2-phenylbenzofuran derivatives were designed and synthesized to determine relevant structural features for the MAO inhibitory activity and selectivity. Methoxy substituents were introduced in the 2-phenyl ring, whereas the benzofuran moiety was not substituted or substituted at the positions 5 or 7 with a nitro group. Substitution patterns on both the phenyl ring and the benzofuran moiety determine the affinity for MAO-A or MAO-B. The 2-(3-methoxyphenyl)-5-nitrobenzofuran **9** was the most potent MAO-B inhibitor ($IC_{50} = 0.024 \mu M$) identified in this series, whereas 7-nitro-2-phenylbenzofuran **7** was the most potent MAO-A inhibitor ($IC_{50} = 0.168 \mu M$), both acting as reversible inhibitors. The number and position of the methoxyl groups on the 2-phenyl ring, have an important influence on the inhibitory activity. Molecular docking studies confirmed the experimental results and highlighted the importance of key residues in enzyme inhibition.

1. Introduction

Monoamine oxidase (MAO) is a flavin adenine dinucleotide (FAD) dependent enzyme responsible for the metabolism of monoamine neurotransmitters, which plays an important role in brain development and function [1].

Two isoforms of the enzymes, namely MAO-A and MAO-B are encoded by distinct genes located on the X chromosome, and are expressed in different amounts in a wide variety of tissues. Moreover, MAO-A and MAO-B have been characterized by their amino acid sequences, three-dimensional structures, inhibitor selectivity, and substrate preferences [2,3].

Serotonin, noradrenaline, and adrenaline are preferential substrates for MAO-A and benzylamine and β -phenylethylamine for MAO-B. Dopamine, tyramine, and tryptamine are common substrates for both

MAO isoforms in most species [4,5]. Because of the role of MAO in the homeostasis of neurotransmitters in the brain, this enzyme has been recognized as an important target for neurological diseases, such as depression, Parkinson's disease (PD) or even Alzheimer's disease (AD) [6].

MAO-A inhibitors are well known as powerful anti-depressants, as well as effective therapeutic agents for social phobia and panic disorder. They are particularly effective in treatment-resistant depression and atypical depression. However, only moclobemide is currently in clinical use. Therefore, the search for novel MAO-A inhibitors certainly remains an attractive topic [7].

MAO-B inhibitors with a propargylamine molecular scaffolding such as selegiline and rasagiline are used in the therapy for neurodegenerative disorders, including PD. They enhance both endogenous dopamine and the one produced from exogenously administered levodopa [8].

* Corresponding authors at: Department of Life and Environmental Sciences, University of Cagliari, 09042 Monserrato, Cagliari, Italy (G.L. Delogu); Center for Research in Molecular Medicine and Chronic Diseases (CIMUS), University of Santiago de Compostela, Avda Barcelona s/n, Campus Vida 15782, Santiago de Compostela, Spain (D. Viña).

E-mail addresses: delogug@unica.it (G.L. Delogu), mdolores.vina@usc.es (D. Viña).

¹ These authors should be considered joint first authors.

While selegiline and rasagiline derivatives are irreversible inhibitors, a new reversible MAO-B inhibitor, safinamide, has been approved by the Food and Drug Administration in 2017 for PD therapy [9].

The reaction of monoamines with MAO results in the generation of H_2O_2 which, when accumulated, mediates neurotoxicity. As far as MAO-B activity is increased in the older brain, MAO-B inhibitors could prevent neuronal damage and secondary injuries by controlling oxidative stress. Therefore, the neuroprotective role of MAO-B inhibitors justifies their potential not only to manage PD but also to AD [10,11].

A benzofuran ring as a core of heterocyclic compounds is an essential structural unit of various biologically active natural medicines and synthetic chemical raw materials. Numerous studies have shown that 2-phenylbenzofurans have strong biological activities such as anti-cancer, anti-bacterial, anti-viral, anti-oxidative, anti-fungal, and anti-microbial. Such a wide range of biological properties, inherent in benzofuran scaffold, justifies the extensive interest in using benzofuran as a building block of pharmacological agents [12].

Recent studies have demonstrated enzymatic inhibition properties of 2-phenylbenzofuran derivatives, for example, against butyrylcholinesterase (BchE) [13–15], and monoamine oxidase (MAO) [16–18]. In general, benzofurans described as MAO inhibitors have a higher selectivity for MAO-B isoform [17,18].

In our efforts to contribute to the development of novel compounds that may be useful in the treatment of disorders associated with MAO, we chose to focus on evaluating the relevance of structural features in the MAOs inhibitory activity. In the present work, we describe the synthesis and biological evaluation and molecular docking of a new series of 2-phenylbenzofuran derivatives with methoxy and/or nitro substitutions.

In our previously studied benzofuran series, 2-(4-methoxyphenyl)-5-nitrobenzofuran was found to be the most active compound, presenting MAO-B selectivity and reversible inhibition ($\text{IC}_{50} = 140 \text{ nM}$) [18,19]. In the present work, we investigated the influence on the enzyme inhibition activity based on the position and number of methoxyl groups' substitutions in the 2-phenyl ring. Besides, we examined the importance of the presence and position of the nitro group on the benzofuran scaffold.

2. Experimental

2.1. Chemistry

2.1.1. General information

Starting materials and reagents were obtained from commercial suppliers and were used without further purification. Melting points (mp) are uncorrected and were determined with a Reichert Kofler thermopan or in capillary tubes in a Büchi 510 apparatus. ^1H NMR and ^{13}C NMR spectra were recorded with a Varian INOVA 500 spectrometer using $\text{DMSO}-d_6$ or CDCl_3 as solvent. Chemical shifts (δ) are expressed in parts per million (ppm) using TMS as an internal standard. Coupling constants J are expressed in hertz (Hz). Spin multiplicities are given as s (singlet), d (doublet), t (triplet) and m (multiplet). Mass spectrometry was carried out with a Saturn 2000 ion-trap coupled with a Varian 3800 gas chromatograph operating under EI conditions. Elemental analyses were performed by a Perkin-Elmer 240B microanalyzer and were within $\pm 0.4\%$ of calculated values in all cases. The analytical results were $\geq 95\%$ purity for all compounds. Flash Chromatography (FC) was performed on silica gel (Merck 60, 230–400 mesh); analytical TLC was performed on precoated silica gel plates (Merck 60 F254). Organic solutions were dried over anhydrous sodium sulfate. Concentration and evaporation of the solvent after reaction or extraction were carried out on a rotary evaporator (Büchi Rotavapor) operating at reduced pressure.

2.1.2. General procedure for the preparation of 2-hydroxybenzylalcohols (Ia–Ic).

Sodium borohydride (6.60 mmol) was added to a stirring solution of

2-hydroxybenzaldehyde (6.60 mmol), in ethanol (20 mL), in an ice bath. The reaction mixture was stirred at room temperature for 1 h. After that, the solvent was removed, 1 N aqueous HCl solution (40 mL) was added to the residue and extracted with diethyl ether. The solvent was evaporated under vacuum to give the desired compounds Ia–Ic [20–23].

2.1.3. General procedure for the preparation of 2-hydroxybenzyltriphenylphosphonium bromide (IIa–IIc).

A mixture of 2-hydroxybenzylalcohol (16.27 mmol) and $\text{PPh}_3\cdot\text{HBr}$ (16.27 mmol) in CH_3CN (40 mL) was stirred under reflux for 2 h. The solid formed was filtered and washed with CH_3CN to give the desired compounds IIa–IIc [20,24,25].

2.1.3.1. 2-hydroxy-3-nitrophenylphosphonium bromide (IIa). It was obtained with a yield of 95%. m.p. 115–117 °C; ^1H NMR (500 MHz, CDCl_3), δ (ppm), J (Hz) = 4.90 (d, 2H, $J = 14.8$, CH_2P), 6.80 (dd, 1H, $J = 7.8$ and 7.6, H-5), 7.20–7.32 (m, 1H, H-6), 7.50 (dd, 1H, $J = 7.8$ and 1.2, H-4), 7.60–7.82 (m, 12H, ArH), 7.85–7.90 (m, 3H, ArH), 10.26 (s, 1H, ArOH) ppm; ^{13}C NMR (125 MHz, CDCl_3), δ (ppm), J (Hz) = 36.58, 117.20, 120.12, 125.10, 131.98, 132.34, 133.46, 133.37, 136.65, 138.20, 152.05 ppm. MS (EI, 70 eV): m/z (%): 496 (98) [$\text{M} + 2$] $^+$, 494 (100) [M] $^+$, 448. Anal. calcd for $\text{C}_{25}\text{H}_{21}\text{BrO}_3\text{P}$: C, 60.74%; H, 4.28%. Found: C, 60.79%; H 4.35.

2.1.4. General procedure for the preparation of 2-phenylbenzofuran (1–18).

A mixture of 2-hydroxybenzyltriphenylphosphonium bromide (1.11 mmol) and benzoyl chloride (1.11 mmol) in a mixed solvent (toluene 20 mL and Et_3N 0.5 mL) was stirred under reflux for 2 h. The precipitate was removed by filtration. The filtrate was concentrated, and the residue was purified by silica gel chromatography (hexane/ EtOAc 9:1) to give the desired compounds.

2.1.4.1. 2-(2-methoxyphenyl)-7-nitrobenzofuran (1). It was obtained with a yield of 47%. m.p. 167–170 °C. ^1H NMR (500 MHz, CDCl_3), δ (ppm), J (Hz) = 4.03 (s, 3H, OCH_3), 7.04 (d, 1H, $J = 8.3$, H-3'), 7.15 (t, 1H, $J = 7.6$, H-5'), 7.33 (t, 1H, $J = 7.9$, H-4'), 7.40 (t, 1H, H-5, $J = 7.9$), 7.45 (s, 1H, H-3), 7.88 (d, 1H, $J = 7.8$, H-6'), 8.24 (d, 1H, $J = 7.8$, H-6), 8.10 (d, 1H, $J = 8.1$, H-4) ppm; ^{13}C NMR (125 MHz, CDCl_3), δ (ppm), J (Hz) = 56.81, 104.63, 113.84, 119.25, 119.62, 122.88, 123.47, 129.85, 129.87, 130.64, 131.26, 134.50, 157.40, 148.51, 153.20 ppm. MS (EI, 70 eV): m/z (%): 269 (100) [M] $^+$, 238, 223, 193, 165. Anal. calcd for $\text{C}_{15}\text{H}_{11}\text{NO}_4$: C, 66.91%; H, 4.12%; N, 5.20%. Found: C, 66.95%; H, 4.16%; N, 5.24%.

2.1.4.2. 2-(3-methoxyphenyl)-7-nitrobenzofuran (2). It was obtained with a yield of 45%. m.p. 115–117 °C. ^1H NMR (500 MHz, CDCl_3), δ (ppm), J (Hz) = 3.95 (s, 3H, OCH_3), 6.98 (d, 1H, $J = 8.2$, H-4'), 7.12 (s, 1H, H-3), 7.38 (m, 2H, H-5' and H-6'), 7.49 (s, 1H, H-2'), 7.55 (dd, 1H, $J = 7.7$ and 1.9, H-5), 7.88 (d, 1H, $J = 7.7$, H-4), 8.12 (d, 1H, $J = 8.0$, H-6) ppm; ^{13}C NMR (125 MHz, CDCl_3), δ (ppm), J (Hz) = 56.10, 104.18, 112.70, 115.98, 118.43, 122.92, 123.48, 128.98, 129.89, 130.68, 131.56, 134.46, 153.22, 158.15, 159.47 ppm. MS (EI, 70 eV): m/z (%): 269 (100) [M] $^+$, 238, 223, 195, 126. Anal. calcd for $\text{C}_{15}\text{H}_{11}\text{NO}_4$: C, 66.91%; H, 4.12%; N, 5.20%. Found: C, 66.96%; H, 4.17%; N, 5.23%.

2.1.4.3. 2-(4-methoxyphenyl)-7-nitrobenzofuran (3). It was obtained with a yield of 51%. m.p. 104–106 °C; ^1H NMR (500 MHz, CDCl_3), δ (ppm), J (Hz) = 3.87 (s, 3H, OCH_3), 6.96 (s, 1H, H-3), 7.00 (d, 2H, $J = 8.9$, H-3' and H-5'), 7.31 (t, 1H, $J = 7.9$, H-5), 7.82 (d, 1H, $J = 6.8$, H-4), 7.88 (d, 2H, $J = 8.9$, H-2' and H-6'), 8.06 (d, 1H, $J = 8.0$, H-6) ppm; ^{13}C NMR (125 MHz, CDCl_3), δ (ppm), J (Hz) = 56.08, 102.93, 114.25, 122.93, 123.32, 123.52, 127.76, 129.94, 130.74, 134.56, 153.25, 158.33, 161.54 ppm. MS (EI, 70 eV): m/z (%): 269 (100) [M] $^+$, 238, 223, 195, 152, 129. Anal. calcd for $\text{C}_{15}\text{H}_{11}\text{NO}_4$: C, 66.91%; H, 4.12%; N, 5.20%.

5.20%. Found: C, 66.95%; H, 4.15%; N, 5.25%.

2.1.4.4. 2-(3,4-dimethoxyphenyl)-7-nitrobenzofuran (4). It was obtained with a yield of 43%. m.p. 175–177 °C; ^1H NMR (500 MHz, CDCl_3), δ (ppm), J (Hz) = 3.96 (s, 3H, OCH_3), 4.01 (s, 3H, OCH_3), 7.04–6.94 (m, 2H, H-3 and H-5'), 7.33 (d, 1H, $J = 7.9$, H-6'), 7.44 (s, 1H, H-2'), 7.56 (dd, 1H, $J = 8.4$ and 1.9 , H-5), 7.85 (d, 1H, $J = 7.61$, H-4), 8.08 (d, 1H, $J = 7.9$, H-6) ppm; ^{13}C NMR (125 MHz, CDCl_3), δ (ppm), J (Hz) = 56.80, 104.16, 111.85, 112.72, 119.84, 122.90, 123.52, 123.98, 129.86, 130.65, 134.52, 149.96, 152.85, 153.24, 158.10 ppm. MS (EI, 70 eV): m/z (%): 299 (100) $[\text{M}]^+$, 268, 253, 237, 220, 210, 181. Anal. calcd for $\text{C}_{16}\text{H}_{13}\text{NO}_5$: C, 64.21%; H, 4.38%; N, 4.68%. Found: C, 64.25%; H, 4.42%; N, 4.70%.

2.1.4.5. 2-(3,5-dimethoxyphenyl)-7-nitrobenzofuran (5). It was obtained with a yield of 46%. m.p. 202–204 °C; ^1H NMR (500 MHz, CDCl_3), δ (ppm), J (Hz) = 3.91 (s, 6H, OCH_3), 6.56 (s, 1H, H-3), 7.09 (m, 3H, H-2' and H-4', H-6'), 7.37 (m, 1H, H-5), 7.89 (d, 1H, $J = 7.7$, H-4), 8.14 (d, 1H, $J = 8.0$, H-6) ppm; ^{13}C NMR (125 MHz, CDCl_3), δ (ppm), J (Hz) = 56.12, 102.84, 104.99, 105.72, 122.93, 123.54, 129.96, 130.77, 133.12, 134.68, 153.26, 157.20, 160.92 ppm. MS (EI, 70 eV): m/z (%): 299 (100) $[\text{M}]^+$, 298, 283, 252, 267, 236, 221, 190. Anal. calcd for $\text{C}_{16}\text{H}_{13}\text{NO}_5$: C, 64.21%; H, 4.38%; N, 4.68%. Found: C, 64.26%; H, 4.44%; N, 4.69%.

2.1.4.6. 2-(3,4,5-trimethoxyphenyl)-7-nitrobenzofuran (6). It was obtained with a yield of 54%. m.p. 145–147 °C; ^1H NMR (500 MHz, CDCl_3), δ (ppm), J (Hz) = 3.93 (s, 3H, OCH_3), 3.99 (s, 6H, OCH_3), 7.07 (s, 1H, H-3), 7.18 (s, 2H, H-2' and H-6'), 7.36 (t, 1H, $J = 8.0$, H-5), 7.87 (d, 1H, $J = 7.7$, H-4), 8.12 (d, 1H, $J = 8.1$, H-6) ppm; ^{13}C NMR (125 MHz, CDCl_3), δ (ppm), J (Hz) = 56.81, 60.67, 103.72, 122.88, 123.47, 126.86, 129.85, 130.63, 134.50, 142.98, 153.20, 154.55, 157.20 ppm. MS (EI, 70 eV): m/z (%): 329 (100) $[\text{M}]^+$, 268, 253, 225, 182. Anal. calcd for $\text{C}_{17}\text{H}_{15}\text{NO}_6$: C, 62.00%; H, 4.59%; N, 4.25%. Found: C, 62.08%; H, 4.63%; N, 4.27%.

2.1.4.7. 7-nitro-2-phenylbenzofuran (7). It was obtained with a yield of 45%. m.p. 118–119 °C; ^1H NMR (500 MHz, CDCl_3), δ (ppm), J (Hz) = 7.13 (s, 1H, H-3), 7.35 (t, 1H, H-4'), 7.53–7.40 (m, 2H, H-4 and H-5), 7.88 (d, 2H, $J = 8.5$, H-3' and H-5'), 7.96 (d, 2H, $J = 8.0$, H-2' and H-6'), 8.12 (dd, 1H, $J = 8.2$, H-6) ppm; ^{13}C NMR (125 MHz, CDCl_3), δ (ppm), J (Hz) = 100.82, 120.48, 122.87, 125.46, 127.45, 128.93, 129.60, 133.28, 133.80, 146.85, 158.61 ppm. MS (EI, 70 eV): m/z (%): 239 (100) $[\text{M}]^+$, 203, 193, 165. Anal. calcd for $\text{C}_{14}\text{H}_9\text{NO}_3$: C, 70.29%; H, 3.79%; N, 5.86%. Found: C, 70.34%; H, 3.85%; N, 6.10%.

2.1.4.8. 2-(2-methoxyphenyl)-5-nitrobenzofuran (8). It was obtained with a yield of 47%. m.p. 174–176 °C; ^1H NMR (500 MHz, CDCl_3), δ (ppm), J (Hz) = 4.04 (s, 3H, OCH_3), 7.05 (d, 1H, $J = 8.3$, H-3') 7.11 (t, 1H, $J = 7.6$, H-5'), 7.40 (t, 1H, $J = 7.8$, H-4'), 7.45 (s, 1H, H-3), 7.57 (d, 1H, $J = 9.0$, H-6'), 8.06 (d, 1H, $J = 7.8$, H-7), 8.21 (d, 1H, $J = 9.0$, H-6), 8.51 (s, 1H, H-4) ppm; ^{13}C NMR (125 MHz, CDCl_3), δ (ppm), J (Hz) = 56.82, 104.12, 113.10, 113.90, 119.30, 119.62, 121.32, 121.59, 125.62, 129.84, 131.25, 140.53, 147.83, 157.52, 158.12 ppm. MS (EI, 70 eV): m/z (%): 269 (100) $[\text{M}]^+$, 222, 195, 152, 131. Anal. calcd for $\text{C}_{15}\text{H}_{11}\text{NO}_4$: C, 66.91%; H, 4.12%; N, 5.20%. Found: C, 66.94%; H, 4.13%; N, 5.24%.

2.1.4.9. 2-(3-methoxyphenyl)-5-nitrobenzofuran (9). It was obtained with a yield of 62%. m.p. 188–189 °C; ^1H NMR (500 MHz, CDCl_3), δ (ppm), J (Hz) = 3.91 (s, 3H, OCH_3), 6.97 (dd, 1H, $J = 72.5$ and 8.0 , H-4'), 7.12 (s, 1H, H-3), 7.36–7.43 (m, 2H, H-2' and H-5'), 7.47 (d, 1H, $J = 7.6$, H-6'), 7.60 (d, 1H, $J = 9.0$, H-7), 8.22 (dd, 1H, $J = 2.4$ and 9.0 , H-6), 8.51 (d, 1H, $J = 2.3$, H-4) ppm; ^{13}C NMR (125 MHz, CDCl_3), δ (ppm), J (Hz) = 55.52, 102.02, 110.70, 111.52, 115.51, 117.32, 117.94, 120.29,

129.63, 130.84, 130.55, 144.43, 157.63, 159.12, 160.21 ppm. MS (EI, 70 eV): m/z (%): 269 (100) $[\text{M}]^+$, 223, 195, 169, 152, 126. Anal. calcd for $\text{C}_{15}\text{H}_{11}\text{NO}_4$: C, 66.91%; H, 4.12%; N, 5.20%. Found: C, 66.92%; H, 4.15%; N, 5.26%.

2.1.4.10. 2-(3,4-dimethoxyphenyl)-5-nitrobenzofuran (10). It was obtained with a yield of 76%. m.p. 207–208 °C; ^1H NMR (500 MHz, CDCl_3), δ (ppm), J (Hz) = 3.96 (s, 3H, OCH_3), 4.01 (s, 3H, OCH_3), 6.97 (d, 1H, $J = 8.4$, H-5'), 7.01 (s, 1H, H-3), 7.37 (d, 1H, $J = 1.8$, H-2'), 7.47 (dd, 1H, $J = 1.9$ and 8.3 , H-6'), 7.57 (d, 1H, $J = 9.0$, H-7), 8.19 (dd, 1H, $J = 2.3$ and 8.9 , H-6), 8.47 (d, 1H, $J = 2.3$, H-4) ppm; ^{13}C NMR (125 MHz, CDCl_3), δ (ppm), J (Hz) = 56.10, 56.12, 100.39, 108.10, 111.22, 111.49, 116.92, 118.64, 119.86, 122.19, 129.93, 144.38, 149.32, 150.42, 157.22, 159.33 ppm. MS (EI, 70 eV): m/z (%): 299 (100) $[\text{M}]^+$, 268, 253, 237, 222. Anal. calcd for $\text{C}_{16}\text{H}_{13}\text{NO}_5$: C, 64.21%; H, 4.38%; N, 4.68%. Found: C, 64.24%; H, 4.45%; N, 4.70%.

2.1.4.11. 2-(3,5-dimethoxyphenyl)-5-nitrobenzofuran (11). It was obtained with a yield of 79%. m.p. 178–180 °C; ^1H NMR (500 MHz, CDCl_3), δ (ppm), J (Hz) = 3.91 (s, 6H, OCH_3), 6.55 (s, 1H, H-3), 7.04 (s, 2H, H-2' and H-6'), 7.14 (s, 1H, H-4'), 7.62 (d, 1H, $J = 9.0$, H-7), 8.24 (dd, 1H, $J = 2.4$ and 8.9 , H-6), 8.56 (d, 1H, $J = 2.4$, H-4) ppm; ^{13}C NMR (125 MHz, CDCl_3), δ (ppm), J (Hz) = 55.51, 101.29, 102.11, 103.42, 111.48, 117.34, 120.24, 129.56, 130.89, 144.33, 157.52, 159.02, 161.24 ppm. MS (EI, 70 eV): m/z (%): 299 (100) $[\text{M}]^+$, 283, 269, 253. Anal. calcd for $\text{C}_{16}\text{H}_{13}\text{NO}_5$: C, 64.21%; H, 4.38%; N, 4.68%. Found: C, 64.18%; H, 4.44%; N, 4.72%.

2.1.4.12. 2-(2,4-dimethoxyphenyl)-5-nitrobenzofuran (12). It was obtained with a yield of 55%. m.p. 186–188 °C; ^1H NMR (500 MHz, CDCl_3), δ (ppm), J (Hz) = 3.78 (s, 3H, OCH_3), 3.99 (s, 3H, OCH_3), 6.64–6.59 (m, 2H, H-3' and H-5'), 7.29 (s, 1H, H-3), 7.55 (d, 1H, $J = 13.7$, H-6'), 7.97 (d, 1H, $J = 8.7$, H-7), 8.17 (d, 1H, $J = 9.0$, H-6), 8.47 (s, 1H, H-4) ppm; ^{13}C NMR (125 MHz, CDCl_3), δ (ppm), J (Hz) = 56.08, 56.82, 100.69, 104.10, 106.32, 113.19, 115.62, 121.32, 121.56, 125.89, 129.53, 140.48, 147.79, 158.12, 160.22, 161.42 ppm. MS (EI, 70 eV): m/z (%): 299 (100) $[\text{M}]^+$, 268, 253, 237, 222. Anal. calcd for $\text{C}_{16}\text{H}_{13}\text{NO}_5$: C, 64.21%; H, 4.38%; N, 4.68%. Found: C, 64.26%; H, 4.46%; N, 4.69%.

2.1.4.13. 2-(3,4,5-trimethoxyphenyl)-5-nitrobenzofuran (13). It was obtained with a yield of 58%. m.p. 250–252 °C; ^1H NMR (500 MHz, CDCl_3), δ (ppm), J (Hz) = 3.93 (s, 3H, OCH_3), 3.99 (s, 6H, OCH_3), 7.11 (s, 1H, H-3), 7.27 (s, 2H, H-2' and H-6'), 7.61 (d, 1H, $J = 9.0$, H-7), 8.23 (d, 1H, $J = 9.0$, H-6), 8.51 (s, 1H, H-4) ppm; ^{13}C NMR (125 MHz, CDCl_3), δ (ppm), J (Hz) = 56.83, 60.74, 103.32, 103.75, 113.25, 121.20, 121.53, 125.82, 126.96, 140.52, 142.99, 154.56, 158.10, 158.61 ppm. MS (EI, 70 eV): m/z (%): 329 (100) $[\text{M}]^+$, 283, 252, 221, 190. Anal. calcd for $\text{C}_{17}\text{H}_{15}\text{NO}_6$: C, 62.00%; H, 4.59%; N, 4.25%. Found: C, 62.07%; H, 4.60%; N, 4.29%.

2.1.4.14. 5-nitro-2-phenylbenzofuran (14). It was obtained with a yield of 40%. m.p. 158–159 °C; ^1H NMR (500 MHz, CDCl_3), δ (ppm), J (Hz) = 7.13 (s, 1H, H-3), 7.44–7.46 (m, 1H, H-4'), 7.48–7.52 (m, 2H, H-3' and H-5'), 7.59 (d, 1H, $J = 9.2$, H-7), 7.88 (d, 2H, $J = 7.6$, H-2' and H-6'), 8.22 (dd, 1H, $J = 2.0$ and 8.8 , H-6), 8.52 (d, 1H, $J = 2.4$, H-4) ppm; ^{13}C NMR (125 MHz, CDCl_3), δ (ppm), J (Hz) = 101.58, 111.42, 117.25, 120.12, 125.28, 128.96, 129.25, 129.62, 129.66, 144.32, 157.58, 159.25 ppm. MS (EI, 70 eV): m/z (%): 239 (100) $[\text{M}]^+$, 203, 193, 165. Anal. calcd for $\text{C}_{14}\text{H}_9\text{NO}_3$: C, 70.29%; H, 3.79%; N, 5.86%. Found: C, 70.35%; H, 3.87%; N, 6.20%.

2.1.4.15. 2-(2-methoxyphenyl)benzofuran (15). It was obtained with a yield of 80%. m.p. 78–79 °C; ^1H NMR (500 MHz, CDCl_3), δ (ppm), J (Hz) = 4.02 (s, 3H, OCH_3), 7.02 (d, 1H, $J = 8.2$, H-3), 7.08–7.10 (m, 1H, H-

3'), 7.21–7.36 (m, 4H, H-5, H-6, H4' and H5'), 7.52 (d, 1H, $J = 8.2$, H-7); 7.60 (d, 1H, $J = 7.5$, H-4); 8.08 (dd, 1H, $J = 1.7$, 7.7H-6') ppm; ^{13}C NMR (125 MHz, CDCl_3), δ (ppm), J (Hz) = 55.43, 106.32, 110.81, 111.05, 119.36, 120.79, 121.07, 122.61, 124.13, 127.05, 129.24, 129.88, 152.16, 153.94, 156.52 ppm. MS (EI, 70 eV): m/z (%): 224 (100) $[\text{M}]^+$, 209, 193. Anal. calcd for $\text{C}_{15}\text{H}_{12}\text{O}_2$: C, 80.34%; H, 5.39%; Found: C, 80.38%; H, 5.45%.

2.1.4.16. 2-(3-methoxyphenyl)benzofuran (16). It was obtained with a yield of 88%. m.p. 49–50 °C; ^1H NMR (500 MHz, CDCl_3), δ (ppm), J (Hz) = 3.90 (s, 3H, OCH_3), 6.91 (ddd, 1H, $J = 0.7$, 2.6 and 8.2, H-4'), 7.03 (s, 1H, H-3); 7.22–7.25 (m, 1H, H-5), 7.28–7.31 (m, 1H, H-2'), 7.36 (t, 1H, $J = 8.2$, H-5'), 7.41–7.42 (m, 1H, H-6), 7.46–7.47 (m, 1H, H-6'), 7.53 (d, 1H, $J = 8.4$, H-7), 7.58–7.59 (m, 1H, H-4) ppm; ^{13}C NMR (125 MHz, CDCl_3), δ (ppm), J (Hz) = 55.3, 101.62, 110.14, 111.16, 114.43, 117.55, 120.97, 122.96, 124.36, 129.14, 129.83, 131.72, 154.84, 155.72, 159.86. ppm. MS (EI, 70 eV): m/z (%): 224(100) $[\text{M}]^+$, 293, 195, 169, 152, 126. Anal. calcd for $\text{C}_{15}\text{H}_{12}\text{O}_2$: C, 80.34%; H, 5.39%; Found: C, 80.33%; H, 5.41%.

2.1.4.17. 2-(3,4-dimethoxyphenyl)benzofuran (17). It was obtained with a yield of 84%. m.p. 120–121 °C; ^1H NMR (500 MHz, CDCl_3), δ (ppm), J (Hz) = 3.96 (s, 3H, OCH_3), 4.02 (s, 3H, OCH_3), 6.94 (s, 1H, H-3), 6.97 (d, 1H, $J = 8.4$, H-5'), 7.24 (td, 1H, $J = 1.14$ and 7.30, H-5), 7.28 (td, 1H, $J = 1.40$ and 7.30, H-2'), 7.41 (d, 1H, $J = 1.98$, H-6'), 7.47 (dd, 1H, $J = 2.00$ and 8.35, H-6), 7.52–7.55 (m, 1H, H-7), 7.57–7.60 (m, 1H, H-4) ppm; ^{13}C NMR (125 MHz, CDCl_3), δ (ppm), J (Hz) = 55.97, 56.01, 100.12, 108.21, 111.04, 114.45, 118.23, 120.76, 122.93, 123.6, 123.97, 129.56, 149.32, 149.61, 154.83, 156.04 ppm. MS (EI, 70 eV): m/z (%): 254 (100) $[\text{M}]^+$, 239, 223, 192. Anal. calcd for $\text{C}_{16}\text{H}_{14}\text{O}_3$: C, 75.57%; H, 5.55%; Found: C, 75.60%; H, 5.60%.

2.1.4.18. 2-(2,4-dimethoxyphenyl)benzofuran (18). It was obtained with a yield of 65%. m.p. 49–52 °C; ^1H NMR (500 MHz, CDCl_3), δ (ppm), J (Hz) = 3.84 (s, 3H, OCH_3), 3.95 (s, 3H, OCH_3), 6.55 (d, 1H, $J = 2.0$, H-3), 6.60 (dd, 1H, $J = 2.5$ and 8.5, H-6), 7.17–7.24 (m, 3H, H-43, H-5 and H-6), 7.48 (d, 1H, $J = 7.5$, H-7), 7.56 (d, 1H, $J = 7.5$, H-4), 7.97 (d, 1H, $J = 8.5$, H-6') ppm; ^{13}C NMR (125 MHz, CDCl_3), δ (ppm), J (Hz) = 55.45, 0.98, 72, 104.23, 104.82, 110.43, 112.74, 120.24, 122.65, 123.59, 127.93, 130.02, 152.42, 153.64, 157.76, 160.88 ppm. MS (EI, 70 eV): m/z (%): 254 (100) $[\text{M}]^+$, 239, 223, 192. Anal. calcd for $\text{C}_{16}\text{H}_{14}\text{O}_3$: C, 75.57%; H, 5.55%; Found: C, 75.39%; H, 5.41%.

2.2. Determination of human MAO (hMAO) isoforms activity

The effects of the tested compounds on the enzymatic activity of hMAO isoforms were evaluated by a fluorimetric method using an Amplex Red MAO assay kit (InvitrogenTM) and MAO isoforms prepared from insect cells (BTI-TN-5B1-4) infected with recombinant baculovirus containing cDNA inserts from MAO-A or MAO-B (Sigma-Aldrich). Briefly, 0.1 mL of sodium phosphate buffer (0.05 M, pH 7.4) containing the tested drugs in several concentrations and adequate amounts of recombinant hMAO-A or hMAO-B required and adjusted to obtain in our experimental conditions the same reaction velocity [165 pmol of *p*-tyramine/min (hMAO-A: 1.1 μg protein; specific activity: 150 nmol of *p*-tyramine oxidized to *p*-hydroxyphenylacetaldehyde/min/mg protein; hMAOB: 7.5 μg protein; specific activity: 22 nmol of *p*-tyramine transformed/min/mg protein)] were placed in each well of a 96-well black plate (MicrotestTM 96 well assay plate, BD Biosciences) and incubated in the dark fluorimeter chamber for 15 min at 37 °C. The reaction was started by adding (final concentrations) 200 μM Amplex Red reagent, 1 U/mL horseradish peroxidase and 1 mM *p*-tyramine. The production of H_2O_2 and, consequently, of resorufin was quantified at 37 °C in a multidetector microplate fluorescence reader (FLX800TM, Bio-Tek Instruments, Inc., Winooski, VT, USA) based on the fluorescence generated

(excitation, 545 nm, emission, 590 nm) over a 15 min period, in which the fluorescence increased linearly.

Control experiments were carried out simultaneously by replacing the tested drugs with appropriate dilutions of the vehicles. In addition, the possible capacity of the above tested drugs for modifying the fluorescence generated in the reaction mixture due to non-enzymatic inhibition (e.g., for directly reacting with Amplex Red reagent) was determined by adding these drugs to solutions containing only the Amplex Red reagent in a sodium phosphate buffer. The specific fluorescence emission (used to obtain the final results) was calculated after subtraction of the background activity, which was determined from wells containing all components except the hMAO isoforms, which were replaced by a sodium phosphate buffer solution [26].

2.3. Reversibility

To evaluate whether compounds **7** and **9** are reversible or irreversible hMAO-A and hMAO-B inhibitors respectively, a dilution method was used [27]. A 100X concentration of the enzyme used in the experiments described above was incubated with a concentration of inhibitor equivalent to 10-fold its IC_{50} value. After 30 min, the mixture was diluted 100-fold and MAO inhibition was determined as above. Reversible inhibitors show linear progress with a slope equal to $\approx 91\%$ of the slope of the control sample, whereas irreversible inhibition reaches only $\approx 9\%$ of this slope. Control tests were performed by pre-incubating and diluting the enzyme in the absence of inhibitor.

2.4. Cytotoxicity

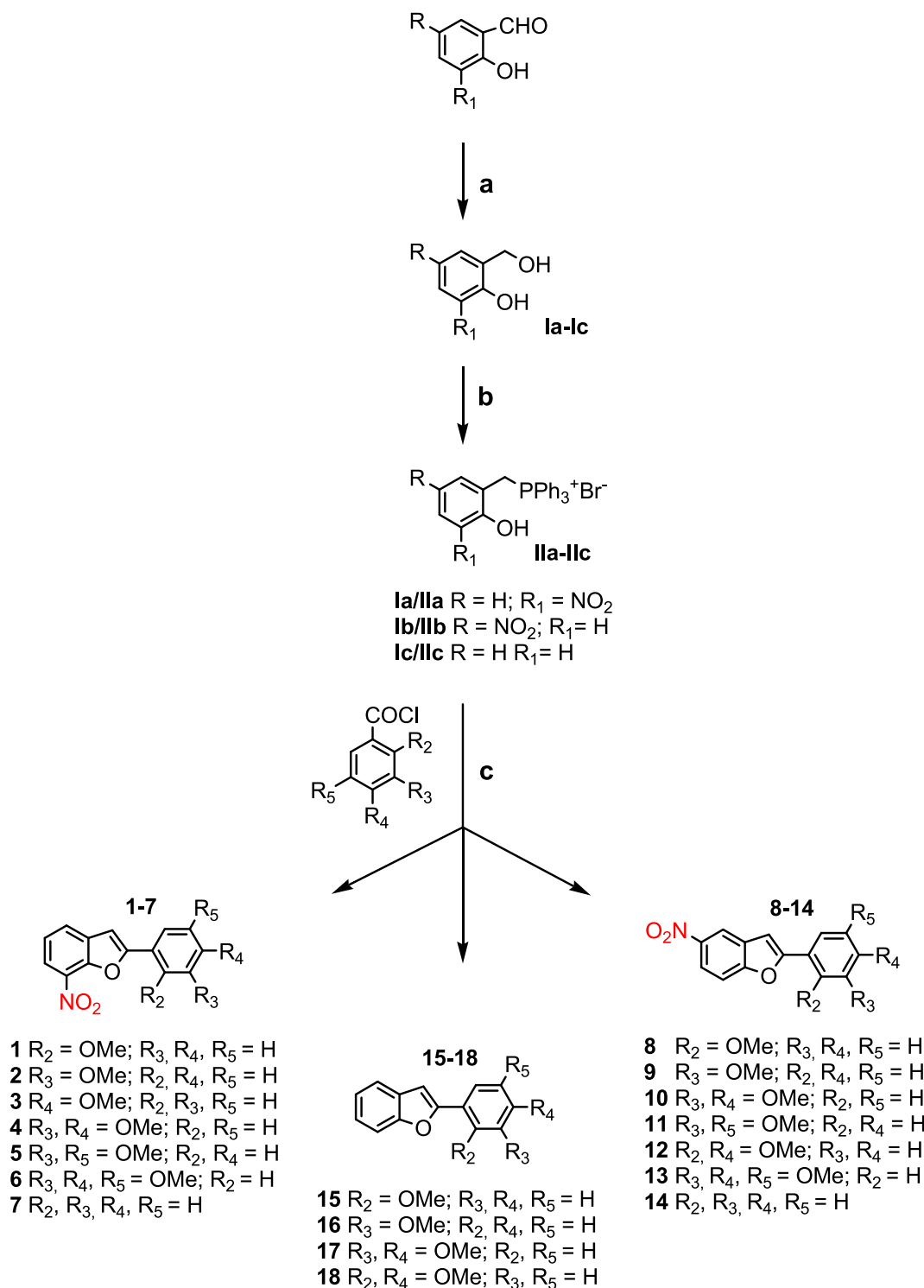
The SH-SY5Y cells grew in a culture medium containing Nutrient Mixture F-12 Ham (Ham's F12) and Minimum Essential Medium Eagle (EMEM) (mixture 1:1) and supplemented with 15% Fetal Bovine Serum (FBS), 1% L-Glutamine, 1% non-essential amino acids (all of them from Sigma-Aldrich S.A.) and 1% of penicillin G/streptomycin sulfate (Gibco, Invitrogen). The cells grew in 75 cm^2 flasks in an incubator (Forma Direct Heat CO_2 , Thermo Electron Corporation), under conditions of saturated humidity with a partial pressure of 5% CO_2 in the air, at 37 °C, until reaching the confluence, 90–95% of the flask surface. To carry out the cytotoxicity assays, the cells were seeded in sterile 96-well plates, with a density of 2×10^5 cells/mL and grown distributed in aliquots of 100 μL for 24 h under the conditions above described [28].

Subsequently, the cultures were treated with the compounds dissolved in DMSO, at 50 or 30 μM concentration (0.5% or 0.3% DMSO/100 μL well) and incubated for 24 h. After this time, cell viability was determined using MTT (5 mg/mL in Hank's). 10 μL of MTT solution were added to each well containing 100 μL of culture medium and the cells were incubated for 2 h as above described. Then, culture medium was removed, 100 μL DMSO/well was added to solve the formazan crystals formed by the viable cells and the absorbance (λ 540 nm) was quantified in a plate reader. The viability (percentage) was calculated as [Absorbance (treatment)/Absorbance (negative control)] 100% [29].

2.5. In silico prediction of ADME properties and metabolic stability

The Molinspiration Cheminformatics software (<https://www.molinspiration.com/>) was used to calculate the physicochemical properties of the 2-phenylbenzofuran derivatives. The octanol/water partition coefficient (LogP), the polar surface area (TPSA), the number of atoms and molecular weight (MW), the number of H-bond acceptors (ON) and H-bond donors (OHNH), the volume (V) and the number of rotatable links (rotb) were calculated, as well as the prediction of the violations of Lipinski rules (n viol) [30]. These results together give an idea of the potential bioavailability of these compounds.

To assess metabolism we performed an *in silico* prediction using the MaxEfficiency mode of GLORY system (<https://acm.zbh.uni-hamburg.de/glory/>) which combines sites of metabolism prediction (SoM)



Scheme 1. Synthesis of 2-phenylbenzofuran derivatives via Wittig reaction. Reagents and conditions: a) NaBH₄, EtOH, 0 °C to rt, 2 h; b) PPh₃ HBr, CH₃CN, 82 °C, 2 h; c) toluene, Et₃N, 110 °C, 2 h.

performed with FAME₂ and a collection of rules for metabolic reactions mediated by the cytochrome P450 enzyme family. A priority score for each predicted metabolite based on the SoM probability of the atoms involved in the transformation and whether the reaction type is common or not let to rank the predicted metabolites for a particular molecule [31,32].

2.6. In vitro blood–brain barrier permeation assay (PAMPA-BBB)

Prediction of the brain penetration was evaluated using the PAMPA-BBB assay, as previously described [33–37]. Solutions were added to 96-well plates using a semi-automatic electronic pipette (CyBi®-SELMA) and UV reading with a microplate spectrophotometer (Multiskan Spectrum, Thermo Electron Co.). Commercial drugs, phosphate buffered saline solution at pH 7.4 (PBS), and dodecane were purchased from Sigma, Aldrich, Acros, and Fluka. Millex filter units (PVDF membrane,

Table 1

IC_{50} values and MAO-B selectivity index (SI) [IC_{50} (MAO-A)]/[IC_{50} (MAO-B)] for the inhibitory effects of test drugs (new compounds and reference inhibitors) on the enzymatic activity of human recombinant MAO isoforms expressed in baculovirus infected BTI insect cells.

Compounds	IC_{50} hMAO-B (μ M)	IC_{50} hMAO-A (μ M)	S.I.
1	> 100	> 100	—
2	0.534 ± 0.037	1.69 ± 0.11	3.16
3	0.342 ± 0.018	0.538 ± 0.11	1.57
4	15.64 ± 2.06	> 100	> 6.39 ^a
5	28.00 ± 3.18	> 100	> 3.57 ^a
6	> 100	> 100	—
7	9.72 ± 0.65	0.168 ± 0.011	0.02
8	29.99 ± 3.68	> 100	> 3.33 ^a
9	0.024 ± 0.003	> 100	> 4,212 ^a
10	> 100	> 100	—
11	> 100	> 100	—
12	1.72 ± 0.27	0.184 ± 0.028	0.11
13	> 100	> 100	—
14	0.551 ± 0.072	> 100	> 181.5 ^a
15	15.80 ± 0.38	**	6.33
16	0.620 ± 0.064	**	161.3
17	4.48 ± 0.20	> 100	> 22.3 ^a
18	4.29 ± 0.29	18.12 ± 1.45	4.23
selegiline	0.017 ± 0.002	68.73 ± 4.20	4,043
clorgyline	61.35 ± 1.13	0.001 ± 0.0003	0.000016
moclobemide	> 100	361.38 ± 19.37	< 3.62 ^a
safinamide [#]	0.060 ± 0.005	90 ± 2.47	1,500

Each IC_{50} value is the mean \pm SEM of three experiments ($n = 3$). [a] Values obtained under the assumption that the corresponding IC_{50} against MAO-A or MAO-B is the highest concentration tested (100 μ M). ** 100 μ M concentration inhibits enzymatic activity by approximately 45–50%. Compounds precipitate at higher concentrations. [#]Safinamide data from ref. [45]x

diameter 25 mm, pore size 0.45 μ m) were acquired from Millipore. The porcine brain lipid (PBL) was obtained from Avanti Polar Lipids. The donor microplate was a 96-well filter plate (PVDF membrane, pore size 0.45 μ m) and the acceptor microplate was an indented 96-well plate, both from Millipore. The acceptor 96-well microplate was filled with 200 μ L of PBS: EtOH (70:30) and the filter surface of the donor plate was impregnated with 4 μ L of PBL in dodecane (20 mg mL⁻¹). Compounds were dissolved in PBS: EtOH (70:30), filtered through a Millex filter, and then added to the donor wells (200 μ L). The donor filter plate was carefully put on the acceptor plate to form a sandwich, which was left undisturbed for 240 min at room temperature. After incubation, the donor plate is carefully removed and the concentration of compounds in the acceptor wells was determined by UV-Vis spectroscopy. Every sample is analyzed at five wavelengths, in four wells and at least in two independent runs, and the results are given as the mean \pm SD. In each experiment, 11 quality control standards of known BBB permeability were included to validate the analysis set.

2.7. Molecular modeling studies

The three-dimensional (3D) protein structures of human MAO-A (PDB id: 2Z5X) [38], and human MAO-B (PDB id: 2 V61) [39] were accessed from the protein data bank. The two-dimensional (2D) sketch of the ligands (6, 7, 9, 12, and 13) was created using the Marvin JS tool (www.chemaxon.com), and subsequently, the 3D-coordinates were generated using Open Babel software [40]. Molecular docking studies were performed using the COACH-D web-server [41], which employs five individual methods to predict the position and conformation of the ligands within the protein-binding site [42,43]. The refinement of the predicted ligand-binding poses was then done using AutoDock Vina [44].

The co-factor FAD in the X-ray structures of the protein was not removed, and the active site was defined by the centroid of co-crystallized ligands that were already present respectively in the protein X-ray structures (2Z5X, 2 V61). The best pose of each compound in

the active site was selected based on binding energy values that were obtained from docking experiments.

3. Results and discussion

3.1. Chemistry

Compounds 1–18 were efficiently synthesized by an intramolecular Wittig reaction (Scheme 1). The desired Wittig reagent was readily prepared from the conveniently substituted 2-hydroxybenzyl alcohol Ia-c and triphenylphosphine hydrobromide (PPh₃HBr) [20–23]. The key step for the formation of the benzofuran moiety was achieved by an intramolecular reaction between 2-hydroxybenzyltriposponium salts IIa-c [20,24,25], and the appropriate benzoylchloride.

The benzofuran structures were then confirmed by employing ¹H NMR, ¹³C NMR, mass spectrometry, and elemental analyses.

3.2. Pharmacology

3.2.1. MAO in vitro inhibition

The results of the hMAO-A and hMAO-B inhibition studies for compounds 1–18 (IC_{50}) and MAO-B selectivity index are reported in Table 1. The test compounds did not show any interference with the reagents used for the biochemical assay. Enzymatic assays revealed that most of the test compounds were moderate to potent hMAO inhibitors at either low micromolar to nanomolar concentrations.

2-(*n*-Methoxyphenyl)benzofurans 15–18 resulted as potent and selective MAO-B inhibitors. For these derivatives, a methoxyl substituent at the *meta* position of the 2-phenyl ring is most favorable for the activity than *ortho* substitution. Therefore, compound 16 is approximately 25 times more potent than 15. However, a double substitution at *meta* and *para* positions (compound 17) leads to similar results than *ortho* and *para* substitutions (compound 18) but major MAO-B selectivity.

An additional substitution with a nitro group at 7 position on the benzofuran moiety leads, in general, to decreased MAO-B activity. Thus, compounds 15 and 17 resulted as more potent MAO-B inhibitors than 1 and 4, respectively. For these 2-(*n*-methoxyphenyl)-7-nitrobenzofurans, the most active compound 3 links the methoxyl group at the *para* position. However, it shows a low selectivity. Besides, it is noteworthy that the absence of methoxyl substituents on 2-phenyl of 7-nitrobenzofuran leads to a potent and quite selective inhibitor of the MAO-A isoform, compound 7, which is 2,151 times more potent than moclobemide.

Conversely, 2-phenyl-5-nitrobenzofuran (14) without methoxyl substituents on the phenyl ring resulted in a potent and selective MAO-B inhibitor. In general, 2-phenyl-5-nitrobenzofuran with only one methoxyl substituent on the phenyl ring resulted as more potent MAO-B inhibitors than the corresponding 2-phenyl-7-nitrobenzofuran. 2-(3-Methoxyphenyl)-5-nitrobenzofuran (9) resulted as the most potent MAO-B inhibitor in the studied series with a potency similar to selegiline.

Increasing the number of methoxyl groups on the phenyl ring, we noticed a decrease in the activity, which is most effective for 2-phenyl-5- or 7-nitrobenzofurans than for 2-phenylbenzofurans. Substitution with three methoxyl groups in *para* and in both *meta* positions on the 2-phenyl ring in compounds 6 and 13, leads to loss of activity.

Also, it is important to point out that the presence of a nitro group at 5 position of the 2-(2,4-dimethoxyphenyl)benzofuran increases its inhibitory activity against both MAO-B and MAO-A. However, a more significant increase is noted against MAO-A. Furthermore, compound 12 is almost 100 times more potent as MAO-A inhibitor than compound 18.

3.3. Reversibility

Reversibility experiments were performed to evaluate the type of inhibition exerted by derivatives 7, the most potent MAO-A inhibitor, and 9, the most potent MAO-B inhibitor in this series. An effective

Table 2

Reversibility results of hMAO-A inhibition for compound 7 and hMAO-B inhibition for compound 9 and reference inhibitors.

Compounds	Slope ($\Delta\text{UF}/t$) [%] ^[a]
7	48.40 \pm 3.50
9	67.95 \pm 2.75
selegiline	9.50 \pm 0.20
clorgyline	8.70 \pm 0.58

^[a] Values represent the mean \pm SEM of $n = 2$ experiments relative to control; data show recovery after dilution of hMAO-A activity incubated with compound 7 or clorgyline and hMAO-B activity incubated with compound 9 or selegiline.

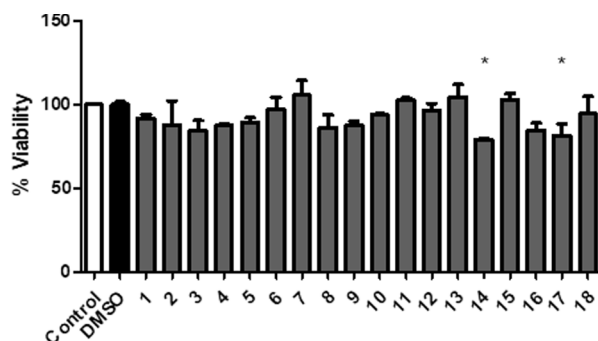


Fig. 1. Cytotoxic activity of compounds 1–18 after 24 h incubation in SH-SY5Y cells. Cell viability was measured as MTT reduction and data were normalized as % of control. Results are expressed as mean \pm SEM from at least 3 different cultures. * $P \leq 0.05$ versus the cells treated with DMSO (0.5%). Comparisons were performed by one-way ANOVA followed by the Dunnett's test.

dilution method was used [27], and selegiline (irreversible MAO-B inhibitor) and clorgyline (irreversible MAO-A inhibitor) were taken as standards. Compounds 7 and 9 resulted as reversible hMAO-A and

hMAO-B inhibitors, respectively (Table 2). Although there is some controversy about the most appropriate type of inhibition for MAO inhibitors, reversible inhibitors appear to have a better safety profile, and they represent an alternative to the irreversible inhibitors currently in therapeutic use.

3.4. Cytotoxicity

The cytotoxic effects of compounds 1–18 were evaluated by using the human neuroblastoma cell line SH-SY5Y. Cells were treated with the compounds at 50 μM concentration and incubated for 24 h. Afterward, the percentage of cell viability was measured as MTT reduction [29].

As depicted in Fig. 1, most of the 2-phenylbenzofuran derivatives evaluated lack cellular toxicity at 50 μM concentration. Only the compounds 14 and 18 appreciably reduced the viability of the SH-SY5Y cells at this concentration. This cytotoxicity disappears with decreasing concentration. Thus, at 30 μM concentration, which is higher than that inhibiting MAO-B in vitro, the viability of the cells after treatment with compounds 14 and 18 was 99.0 ± 6.6 and $84.3 \pm 5.6\%$. At this concentration, no statistically significant differences with the viability of the control were observed ($P < 0.05$).

3.5. In silico and in vitro prediction of ADME properties

In silico calculations using the Molinspiration Cheminformatics software (<https://www.molinspiration.com/>) showed that all the 2-phenylbenzofurans studied have adequate physicochemical properties to display good bioavailability, and none of them violate the Lipinski rule of five (Table 3). The main differences between our derivatives and the reference inhibitors are noted in the LogP and TPSA values. In general, LogP is much higher concerning the reference compounds moclobemide, selegiline and safinamide but comparable to clorgyline. For compounds linking a nitro group, the value of TPSA is comparable to that of the reference inhibitors moclobemide or safinamide.

Moreover, the ability of new 2-phenylbenzofuran derivatives to cross the blood–brain barrier (BBB) was predicted by the in vitro parallel artificial membrane permeability assay for the BBB (PAMPA-BBB),

Table 3

Structural properties of 2-phenylbenzofuran derivatives 1–18, and reference compounds.

Compounds	Log P^a	TPSA (\AA^2) ^b	MW (Da) ^c	$n\text{OH}^d$	$n\text{OHNH}^d$	Volume ^e	Lipinski ^f
1	4.10	68.28	269.26	5	0	229.89	0
2	4.12	68.20	269.26	5	0	229.89	0
3	4.15	68.20	269.26	5	0	229.89	0
4	3.74	77.43	299.28	6	0	255.44	0
5	4.13	77.43	299.28	6	0	255.44	0
6	3.72	86.67	329.31	7	0	280.98	0
7	4.09	58.96	239.23	4	0	204.35	0
8	4.12	68.20	269.26	5	0	229.89	0
9	4.05	104.79	269.26	5	0	229.89	0
10	3.76	77.43	299.28	6	0	255.44	0
11	4.16	77.43	299.28	6	0	255.44	0
12	4.16	77.43	299.28	6	0	255.44	0
13	3.75	86.67	329.31	7	0	280.98	0
14	4.12	58.96	239.23	4	0	204.35	0
15	4.19	22.37	224.26	2	0	206.56	0
16	4.21	22.37	224.26	2	0	206.56	0
17	3.83	31.61	254.28	3	0	232.10	0
18	4.22	31.61	254.28	3	0	232.10	0
clorgyline	3.74	12.47	272.18	2	0	238.91	0
moclobemide	1.69	41.57	268.74	4	1	240.70	0
selegiline	2.64	3.24	187.29	1	0	202.64	0
safrinamide	2.91	64.36	320.35	4	3	279.04	0

^a Log P – expressed as the logarithm of octanol/water partition coefficient.

^b TPSA – topological polar surface area.

^c MW – molecular weight.

^d Number of hydrogen bond acceptors ($n\text{OH}$) and donors ($n\text{OHNH}$).

^e Molecular volume.

^f Number of violations of Lipinski's rules.

Table 4
CNS-Permeability prediction based on the PAMPA-BBB assay (P_e , 10^{-6} cm s $^{-1}$).

Compounds	P_e (10^{-6} cm s $^{-1}$)	CNS Prediction
3	8.8 ± 0.16	CNS +
4	9.3 ± 0.27	CNS +
5	10.2 ± 0.05	CNS +
6	7.1 ± 0.71	CNS +
7	8.6 ± 0.02	CNS +
16	0.7 ± 0.05	CNS -
17	9.4 ± 0.01	CNS +
18	2.1 ± 0.08	CNS + / -

^aResults are the mean \pm SD of at least two independent experiments, where every sample was analyzed at five wavelengths in four different wells.

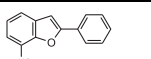
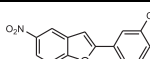
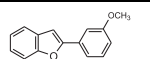
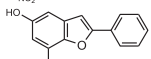
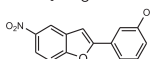
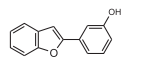
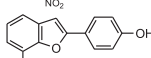
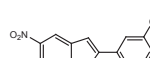
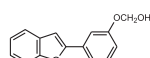
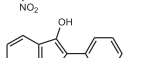
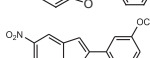
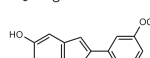
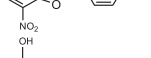
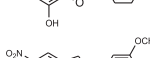

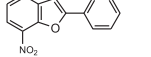
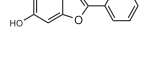
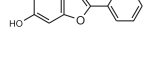
described by Di *et al.* [33] and then adapted by us for testing molecules with limited water-solubility [34–37]. To measure the passive CNS-permeation of new compounds we selected a mixture of PBS:EtOH (70:30) as solvent. In these conditions, the 2-phenylbenzofuran derivatives 3–7 and 16–18 gave solutions with a suitable UV-signal to be detected in the experiment, while the rest of the compounds showed

little solubility and/or too low UV-response, and therefore, they could not be tested. In each experiment, 11 commercial drugs of known brain permeability were also tested and their permeability values normalized to the reported PAMPA-BBB data. As previously established by Di *et al.* [33], compounds with $P_e > 4.0 \cdot 10^{-6}$ cm s $^{-1}$ would cross the BBB (cns +), whereas those displaying $P_e < 2.0 \cdot 10^{-6}$ cm s $^{-1}$ would not reach the CNS (cns-). Between these values, the predicted CNS permeability was uncertain (cns +/-) [33]. As shown in table 4, the 2-phenylbenzofuran derivatives 3–7 and 17 were predicted to be CNS-permeable, whereas 16 and 18 could experience difficulties crossing the BBB.

3.6. In silico metabolism

With the aim of advancing further on the potential therapeutic success of these series of 2-phenylbenzofuran derivatives we perform an in silico prediction of the metabolism for the most potent compounds 7, 9 and 16 corresponding to different series. GLORY combines SoM prediction with FAME₂ and a new collection of rules for metabolic reactions mediated by the cytochrome P450 enzyme family. The importance of CYPs to drug discovery is clear from the observation that many drugs are

Table 5
The most possible metabolites for compounds 7, 9 and 16.

Comp.	structure	score	Comp.	Structure	score	Comp.	structure	score
7			9			16		
M7.1		2.43	M9.1		4.38	M16.1		4.34
M7.2		2.04	M9.2		4.38	M16.2		4.34
M7.3		1.92	M9.3		1.66	M16.3		2.92
M7.4		1.87	M9.4		1.61	M16.4		2.51
M7.5		1.84	M9.5		1.43	M16.5		2.32

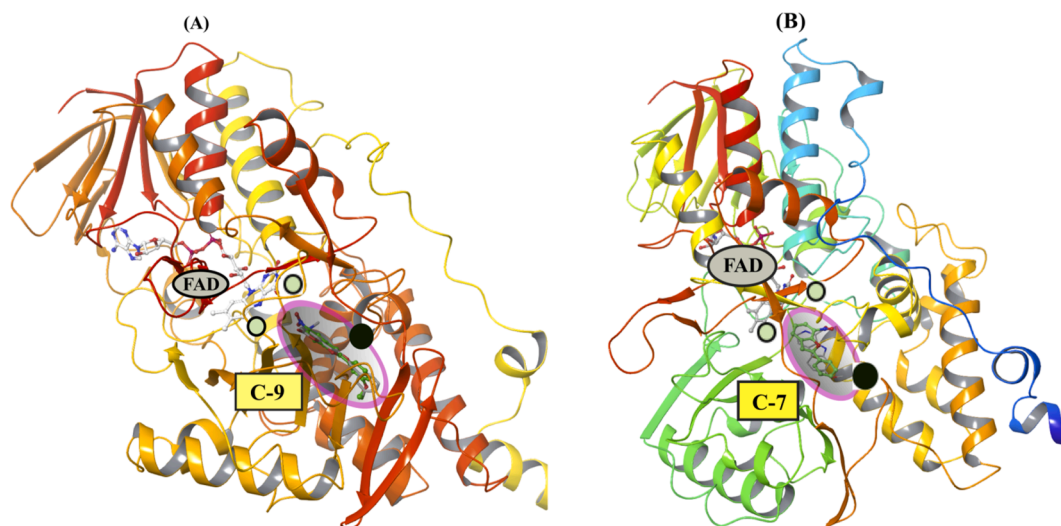


Fig. 2. Structures of human MAO complexes with top ranked ligands. (A) hMAO-B in complex with compound 9 (C-9), and (B) hMAO-A complex with compound 7 (C-7). The binding site of the ligands is represented as the region enclosed within the pink oval. The residues forming aromatic cage are shown as green circle, and the residue determining ligand specificity is shown as black-filled circle. (For interpretation of the references to colour in this figure legend, the reader is referred to the web version of this article.)

Table 6

Predicted binding free energy (ΔG) for the ligands under investigation. The ligand with better binding energy and (IC_{50}) value are highlighted in bold.

Ligand	IC_{50} (μM)		ΔG (kcal/mol)	
	MAO-B	MAO-A	MAO-B	MAO-A
6	> 100	> 100	-7.1	-0.4
7	9.72	0.168	-7.6	-8.2
9	0.024	>100	-8.7	-5.9
12	1.72	0.184	-7.5	-7.9
13	> 100	> 100	-6.2	-0.3
selegiline	0.017	68.73	-7.1	-6.8
clorgyline	61.35	0.001	-7.3	-7.2
moclobemide	> 100	361	-7.2	-8.1

metabolized by CYPs. Results of GLORY suggest the most probably sites of metabolism (SoM). The predicted metabolites for the most active compounds in each series ranked by empirical probability scores are described in table 5.

3.7. Molecular docking

Molecular docking is an important tool used in drug discovery, which has been successfully applied to identify promising inhibitors against protein complexes associated to various diseases [46–48]. Here, molecular docking studies for the different ligand–protein complexes (Fig. 2) were performed to provide insights into ligand's selective

inhibitory profile against the two investigated enzymes (hMAO-B, hMAO-A). The most significant difference between the two enzymes can be noted in the structure of their active site cavities; a single cavity (with $\sim 500 \text{ \AA}^3$ volume) in hMAO-A, while a bipartite cavity (entrance $\sim 300 \text{ \AA}^3$ volume, substrate cavity $\sim 400 \text{ \AA}^3$ volume) in hMAO-B.

The computational docking results for ligands studied revealed that they all bind non-covalently to the enzyme. The docked conformation of the top-ranked ligand complexes superimposed nicely with the X-ray structure ligands (supplementary information Fig. S1). The binding free energies of investigated ligands against the two enzymes are shown Table 6.

Among the 2-phenylbenzofuran derivatives, compound 9 displayed better binding affinity to hMAO-B, while compound 7 to hMAO-A. The docking results were in good agreement with the experimental data (Table 6). Furthermore, the binding free energy trend among the ligands for both the proteins was consistent with the noted experimental trend (IC_{50}) values.

The top-ranked docked conformation of compound 9 bound to hMAO-B protein (Fig. 3A, Fig. 3B), revealed hydrophobic interactions between the nitro group (in position 5 of scaffold) and residues Tyr 398 and Tyr 435. These two residues, together with FAD, form an aromatic cage in the substrate cavity region [49]. Further, we also found phenyl ring of ligand interacting with residues Tyr 326 and Ile 199: the former known to be involved in substrate specificity [4], and the latter acting as gate [50] between the entrance and substrate-binding cavities of hMAO-

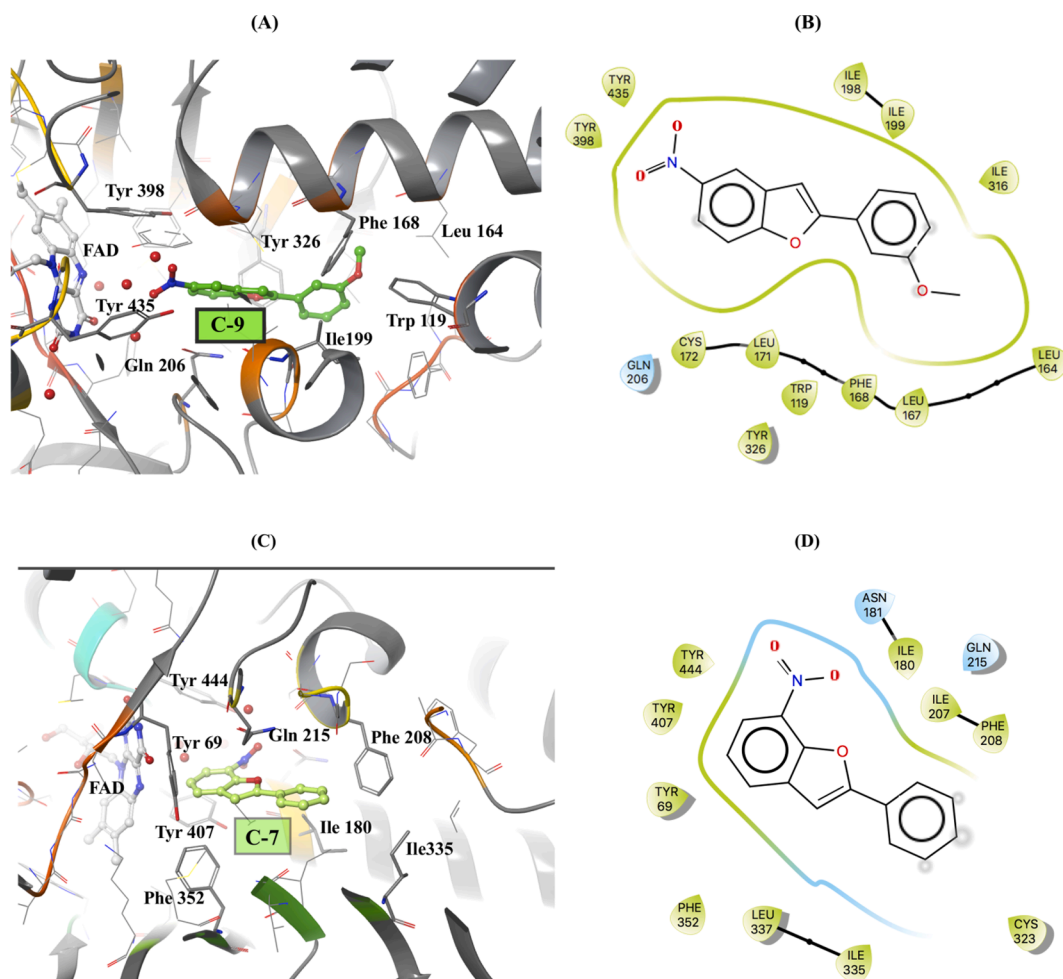


Fig. 3. Zoomed view of predicted docked positions for the top ligands bound to the MAO protein. In (A), and (B) the docked position and interacting picture of compound 9 bound to hMAO-B protein is shown. In (C), and (D) is shown the docked position and interacting picture of compound 7 bound to hMAO-A. In (B), and (D) the polar residues are shown in parrot green, and non-polar residues in cyan. (For interpretation of the references to colour in this figure legend, the reader is referred to the web version of this article.)

B protein. The methoxy substituent of the ligand was found to be involved in hydrophobic interactions with residues Leu 164, Leu 167, and Phe 168. Compound **12**, which shares the same nitro group position as compound **9**, but has additional methoxy substituent, resulted in a similar docked orientation but was more distant from the aromatic cage residues (supplementary information Fig. S2).

Concerning the hMAO-A protein and among the studied derivatives, compound **7** displayed better binding energy (Table 4), and the top-ranked docked conformation shown in Fig. 3C and 3D. The nitro group of compound **7** was involved in hydrophobic interaction with Tyr 407 (aromatic cage), Asn 181, and Gln 215. Further, the phenyl-ring of compound **7** formed strong hydrophobic interactions with residues Ile 180, Phe 208, Cys 323, Ile 335, and Leu 337. Indeed, the critical role of residue Ile 335 in determining substrate and inhibitor specificities have been reported previously [4].

Compound **7** (Fig. 3D) differs from **9** (Fig. 3B) in the nitro group position and also lacks methoxy substituent in the phenyl-ring. The compounds **12** and **9** resulted in a docked orientation with the methoxy group towards the aromatic cage, and nitro group at the other end (supplementary information Fig. S3). The docking results suggest that interaction of the nitro group with the aromatic cage residues can be the reason for better affinity displayed by compound **7**, concerning the other ligands. Further the docking results of ligands with three methoxy substituents in the 2-phenyl ring (compound **6**, compound **13**) indicated unfavourable binding with the hMAO-A enzyme. The reason for unfavourable binding could be related unfavorable contacts displayed by methoxy substituents with key residues: Phe 352, Ile 335, and Gln 215. Indeed, this observation is consistent with a previous docking study [51], wherein the addition of other methoxy groups in the ligand resulted in unfavourable binding characteristics to hMAO-A enzyme. In summary, docking results were consistent with the reported experimental IC₅₀ values for the 2-phenylbenzofuran derivatives. Furthermore, molecular insights into ligand interaction with key residues of the protein facilitating the formation of stable protein–ligand complexes have been illustrated.

4. Conclusion

We have used the Wittig reaction as a key step for the efficient and general synthesis of a series of 2-phenylbenzofuran derivatives. Substitution patterns on both the phenyl ring and the benzofuran moiety determine MAO-A or MAO-B activity. Mainly, a nitro substituent at position 7 of the 2-phenylbenzofuran resulted in more potent MAO-A inhibitors, whereas at position 5 increased the activity MAO-B. Increasing the methoxy groups (2 or 3) on the phenyl rings resulted in a decrease in the activity against the MAO enzyme. These *n*-nitro-2-phenylbenzofurans inhibit MAO-A or MAO-B activity in a reversible manner. All the investigated derivatives lacked toxicity at concentrations higher than those showing activity on MAO isoforms. Further, they possess physicochemical properties to display good bioavailability and many of them were predicted to be CNS-permeable in a PAMPA-BBB assay. Finally, docking studies provided molecular insights that helped explain the structure–activity relationships of this type of compound.

In conclusion, these results could encourage further studies to consider this type of benzofuran derivatives for designing molecules with improved and selective inhibition action against the MAO enzymes.

Declaration of Competing Interest

The authors declare that they have no known competing financial interests or personal relationships that could have appeared to influence the work reported in this paper.

Acknowledgements

The financial support (ED431G 2019/02) from the Xunta de Galicia

(Centro singular de investigación de Galicia accreditation 2019-2022) and the European Union (European Regional Development Fund - ERDF), is gratefully acknowledged. The present work was partially supported by FIR (Fondo Integrativo per la Ricerca – annualità 2018) University of Cagliari. G. L. Delogu is grateful to R. Mascia (University of Cagliari) for his technical assistance. M.I.R.-F. thanks the financial support from Spanish Ministry of Science, Innovation and Universities (grant RTI2018-093955-B-C21) and General Council for Research and Innovation of the Community of Madrid / European Structural Funds (grant B2017/BMD-3827 - NRF24ADCM).

Appendix A. Supplementary data

Supplementary data to this article can be found online at <https://doi.org/10.1016/j.bioorg.2020.104616>.

References

- [1] R.R. Ramsay, Monoamine Oxidases: The Biochemistry of the Proteins As Targets in Medicinal Chemistry and Drug Discovery, *Curr. Top. Med. Chem.* 12 (2012) 2189–2209, <https://doi.org/10.2174/156802612805219978>.
- [2] L. De Colibus, M. Li, C. Binda, A. Lustig, D.E. Edmondson, A. Mattevi, Three-dimensional structure of human monoamine oxidase A (MAO A): Relation to the structures of rat MAO A and human MAO B, *Proceedings of the National Academy of Sciences* 102 (2005) 12684–12689, <https://doi.org/10.1073/pnas.0505975102>.
- [3] C. Binda, M. Li, F. Hubalek, N. Restelli, D.E. Edmondson, A. Mattevi, Insights into the mode of inhibition of human mitochondrial monoamine oxidase B from high-resolution crystal structures, *Proceedings of the National Academy of Sciences* 100 (2003) 9750–9755, <https://doi.org/10.1073/pnas.1633804100>.
- [4] R.M. Geha, I. Rebrin, K. Chen, J.C. Shih, Substrate and Inhibitor Specificities for Human Monoamine Oxidase A and B Are Influenced by a Single Amino Acid, *J. Biol. Chem.* 276 (2001) 9877–9882, <https://doi.org/10.1074/jbc.M006972200>.
- [5] N.A. Garrick, D.L. Murphy, Species differences in the deamination of dopamine and other substrates for monoamine oxidase in brain, *Psychopharmacology* 72 (1980) 27–33, <https://doi.org/10.1007/bf00433804>.
- [6] S. Carradori, D. Secchi, J.P. Petzer, MAO inhibitors and their wider applications: a patent review *Expert Opin. Ther. Pat.* 28 (2018) 211–226, <https://doi.org/10.1080/13543776.2018.1427735>.
- [7] C. Ziegler, K. Domschke, Epigenetic signature of MAOA and MAOB genes in mental disorders, *J. Neural Transm.* 125 (2018) 1581–1588, <https://doi.org/10.1007/s00702-018-1929-6>.
- [8] S.H. Fox, R. Katzenschlager, S.-Y. Lim, B. Barton, R.M.A. de Bie, K. Seppi, M. Coelho, C. Sampaio, International Parkinson and movement disorder society evidence-based medicine review: Update on treatments for the motor symptoms of Parkinson's disease *Mov. Disord.* 33 (2018) 1248–1266, <https://doi.org/10.1002/mds.27372>.
- [9] H.A. Blair, S. Dhillon, Safinamide: A Review in Parkinson's Disease *CNS Drugs*, 31 (2017) 169–176, [10.1007/s40263-017-0408-1](https://doi.org/10.1007/s40263-017-0408-1).
- [10] D.E. Edmondson, C. Binda, Monoamine Oxidases, *Structure and Function, Membrane Protein Complexes*, 2018, pp. 117–139.
- [11] S. Nave, R.S. Doody, M. Boada, T. Grimmer, J.-M. Savola, P. Delmar, M. Pauly-Evers, T. Nikolcheva, C. Czech, E. Borroni, B. Ricci, J. Dukart, M. Mannino, T. Carey, E. Moran, I. Gilaberte, N.M. Muelhardt, I. Gerlach, L. Santarelli, S. Ostrowitzki, P. Pontoura, K. Lancôt, Sembragiline in Moderate Alzheimer's Disease: Results of a Randomized, Double-Blind, Placebo-Controlled Phase II Trial (MAYflower RoAD), *J. Alzheimer's Dis.* 58 (2017) 1217–1228, <https://doi.org/10.3233/jad-161309>.
- [12] Y.-H. Miao, Y.-H. Hu, J. Yang, T. Liu, J. Sun, X.-J. Wang, Natural source, bioactivity and synthesis of benzofuran derivatives, *RSC Advances* 9 (2019) 27510–27540, <https://doi.org/10.1039/c9ra04917g>.
- [13] A. Kumar, F. Pintus, A. Di Petrillo, R. Medda, P. Caria, M.J. Matos, D. Vina, E. Pieroni, F. Delogu, B. Era, G.L. Delogu, A. Fais, Novel 2-phenylbenzofuran derivatives as selective butyrylcholinesterase inhibitors for Alzheimer's disease, *Sci. Rep.* 8 (2018) 4424, <https://doi.org/10.1038/s41598-018-22747-2>.
- [14] G.L. Delogu, M.J. Matos, M. Fanti, B. Era, R. Medda, E. Pieroni, A. Fais, A. Kumar, F. Pintus, 2-Phenylbenzofuran derivatives as butyrylcholinesterase inhibitors: Synthesis, biological activity and molecular modeling, *Bioorg. Med. Chem. Lett.* 26 (2016) 2308–2313, <https://doi.org/10.1016/j.bmcl.2016.03.039>.
- [15] A. Fais, A. Kumar, R. Medda, F. Pintus, F. Delogu, M.J. Matos, B. Era, G.L. Delogu, Synthesis, molecular docking and cholinesterase inhibitory activity of hydroxylated 2-phenylbenzofuran derivatives, *Bioorg. Chem.* 84 (2019) 302–308, <https://doi.org/10.1016/j.bioorg.2018.11.043>.
- [16] L.H.A. Prins, J.P. Petzer, S.F. Malan, Inhibition of monoamine oxidase by indole and benzofuran derivatives, *Eur. J. Med. Chem.* 45 (2010) 4458–4466, <https://doi.org/10.1016/j.ejmech.2010.07.005>.
- [17] G.L. Delogu, F. Pintus, L. Mayán, M.J. Matos, S. Vilar, J. Munín, J.A. Fontenla, G. Hripsak, F. Borges, D. Viña, MAO inhibitory activity of bromo-2-phenylbenzofurans: synthesis, in vitro study, and docking calculations, *MedChemComm* 8 (2017) 1788–1796, <https://doi.org/10.1039/c7md00311k>.
- [18] G. Ferino, E. Cadoni, M.J. Matos, E. Quezada, E. Uriarte, L. Santana, S. Vilar, N. P. Tatonetti, M. Yáñez, D. Viña, C. Picciau, S. Serra, G. Delogu, MAO Inhibitory

- Activity of 2-Arylbenzofurans versus 3-Arylcoumarins: Synthesis, in vitro Study, and Docking Calculations, *ChemMedChem* 8 (2013) 956–966, <https://doi.org/10.1002/cmdc.201300048>.
- [19] S. Carradori, R. Silvestri, New Frontiers in Selective Human MAO-B Inhibitors, *J. Med. Chem.* 58 (2015) 6717–6732, <https://doi.org/10.1021/jm501690r>.
- [20] B. Wendt, H. Riem Ha, M. Hesse, *Helv. Chim. Acta* 85 (2002) 2990–3001, [https://doi.org/10.1002/1522-2675\(200209\)85:9<2990::Aid-hlca2990>3.0.Co;2-r](https://doi.org/10.1002/1522-2675(200209)85:9<2990::Aid-hlca2990>3.0.Co;2-r).
- [21] C. Ducho, S. Wendicke, U. Görbig, J. Balzarini, C. Meier, 3,5-Di-(tert-Butyl)-6-fluoro-cycloSal-d4TMP—A Pronucleotide with a Considerably Improved Masking Group *Eur. J. Org. Chem.* 2003 (2003) 4786–4791, <https://doi.org/10.1002/ejoc.200300537>.
- [22] C. Meier, E. De Clercq, J. Balzarini, Nucleotide Delivery from cycloSaligenyl-3'-azido-3'-deoxythymidine Monophosphates (cycloSal-AZTMP), *Eur. J. Org. Chem.* 1998 (1998) 837–846, [https://doi.org/10.1002/\(sici\)1099-0690\(199805\)1998:5<837::Aid-ejoc837>3.0.Co;2-7](https://doi.org/10.1002/(sici)1099-0690(199805)1998:5<837::Aid-ejoc837>3.0.Co;2-7).
- [23] Y. Noma, H. Takahashi, Y. Asakawa, Biotransformation of terpene aldehydes by *Euglena gracilis* Z, *Phytochemistry* 30 (1991) 1147–1151, [https://doi.org/10.1016/S0031-9422\(00\)95192-6](https://doi.org/10.1016/S0031-9422(00)95192-6).
- [24] D.B. Yogesh, D.B. Shenoy, S.K. Agarwal, T. Menaka, G.R. Srinivasa, G. Nagaraja, U. S.S. Kumar, Synthesis, antibacterial and antifungal properties of newer (2-butyl-5-amino-3-benzofuranyl)-4-methoxy phenyl methanone heterocyclic and isoxazolic acids, *J. Chem. Pharm. Res.* 5 (2013) 184–190.
- [25] L. Capuano, A. Ahlhelm, H. Hartmann, New syntheses of 2-acylbenzofurans, 2-acylindoles, 2-indolylcarboxylates and 2-quinolones by intramolecular Wittig reaction, *Chem. Ber.* 119 (1986) 2069–2074.
- [26] M. Yáñez, N. Fraiz, E. Cano, F. Orallo, Inhibitory effects of cis- and trans-resveratrol on noradrenaline and 5-hydroxytryptamine uptake and on monoamine oxidase activity, *Biochem. Biophys. Res. Commun.* 344 (2006) 688–695, <https://doi.org/10.1016/j.bbrc.2006.03.190>.
- [27] R.A. Copeland, Evaluation of enzyme inhibitors in drug discovery. A guide for medicinal chemists and pharmacologists, *Methods Biochem. Anal.* 46 (2005) 1–265.
- [28] F. Rodríguez-Enríquez, M.C. Costas-Lago, P. Besada, M. Alonso Pena, I. Torres-Terán, D. Viña, J.A. Fontenla, M. Sturlese, S. Moro, E. Quezada, C. Terán, Novel coumarin-pyridazine hybrids as selective MAO-B inhibitors for the Parkinson's disease therapy, *Bioorganic Chemistry* 104 (2020), <https://doi.org/10.1016/j.bioorg.2020.104203>.
- [29] Y. Liu, D.A. Peterson, H. Kimura, D. Schubert, Mechanism of cellular 3-(4,5-dimethylthiazol-2-yl)-2,5-diphenyltetrazolium bromide (MTT) reduction, *J. Neurochem* 69 (1997) 581–593, <https://doi.org/10.1046/j.1471-4159.1997.69020581.x>.
- [30] C.A. Lipinski, F. Lombardo, B.W. Dominy, P.J. Feeney, Experimental and computational approaches to estimate solubility and permeability in drug discovery and development settings IPII of original article: S0169-409X(96)00423-1. The article was originally published in *Advanced Drug Delivery Reviews* 23 (1997) 3–25. 1 *Adv. Drug Del. Rev.* 46 (2001) 3–26, [https://doi.org/10.1016/S0169-409X\(00\)00129-0](https://doi.org/10.1016/S0169-409X(00)00129-0).
- [31] C. de Bruyn Kops, C. Stork, M. Šícho, N. Kochev, D. Svozil, N. Jeliakova, J. Kirchmair, GLORY: Generator of the Structures of Likely Cytochrome P450 Metabolites Based on Predicted Sites of Metabolism, *Front. Chem.* 7 (2019) 402, <https://doi.org/10.3389/fchem.2019.00402>.
- [32] C. Stork, G. Embruch, M. Šícho, C. de Bruyn Kops, Y. Chen, D. Svozil, J. Kirchmair, NERDD: a web portal providing access to in silico tools for drug discovery, *Bioinformatics* (2020), <https://doi.org/10.1093/bioinformatics/btz695>.
- [33] L. Di, E.H. Kerns, K. Fan, O.J. McConnell, G.T. Carter, High throughput artificial membrane permeability assay for blood–brain barrier, *Eur. J. Med. Chem.* 38 (2003) 223–232, [https://doi.org/10.1016/S0223-5234\(03\)00012-6](https://doi.org/10.1016/S0223-5234(03)00012-6).
- [34] C. Herrera-Arozamena, M. Estrada-Valencia, C. Pérez, L. Lagartera, J.A. Morales-García, A. Pérez-Castillo, J.F. Franco-Gonzalez, P. Michalska, P. Duarte, R. León, M. G. López, A. Mills, F. Gago, Á.J. García-Yagüe, R. Fernández-Ginés, A. Cuadrado, M.I. Rodríguez-Franco, Tuning melatonin receptor subtype selectivity in oxadiazolone-based analogues: Discovery of QR2 ligands and NRF2 activators with neurogenic properties, *Eur. J. Med. Chem.* 190 (2020), 112090, <https://doi.org/10.1016/j.ejmech.2020.112090>.
- [35] C. Herrera-Arozamena, M. Estrada-Valencia, O. Martí-Marí, C. Pérez, M. de la Fuente Revenga, C.A. Villalba-Galea, M.I. Rodríguez-Franco, Optical control of muscular nicotinic channels with azocuroniums, photoswitchable azobenzenes bearing two N-methyl-N-carbocyclic quaternary ammonium groups, *Eur. J. Med. Chem.* 200 (2020) 1–14, <https://doi.org/10.1016/j.ejmech.2020.112403>.
- [36] M. De La Fuente Revenga, N. Fernández-Sáez, C. Herrera-Arozamena, J.A. Morales-García, S. Alonso-Gil, A. Pérez-Castillo, D.-H. Caignard, S. Rivara, M.I. Rodríguez-Franco, Novel N-acetyl bioisosteres of melatonin: Melatonergic receptor pharmacology, physicochemical studies, and phenotypic assessment of their neurogenic potential, *J. Med. Chem.* 58 (2015) 4998–5014, <https://doi.org/10.1021/acs.jmedchem.5b00245>.
- [37] M. De La Fuente Revenga, C. Pérez, J.A. Morales-García, S. Alonso-Gil, A. Pérez-Castillo, D.H. Caignard, M. Yáñez, A.M. Gamo, M.I. Rodríguez-Franco, Neurogenic potential assessment and pharmacological characterization of 6-Methoxy-1,2,3,4-tetrahydro- β -carboline (Pinoline) and Melatonin-Pinoline Hybrids, *ACS Chem. Neurosci.* 6 (2015) 800–810, <https://doi.org/10.1021/acschemneuro.5b00041>.
- [38] S.Y. Son, J. Ma, Y. Kondou, M. Yoshimura, E. Yamashita, T. Tsukihara, Structure of human monoamine oxidase A at 2.2-Å resolution: The control of opening the entry for substrates/inhibitors, *Proceedings of the National Academy of Sciences*, 105 (2008) 5739–5744, <https://doi.org/10.1073/pnas.0710626105>.
- [39] C. Binda, J. Wang, L. Pisani, C. Caccia, A. Carotti, P. Salvati, D.E. Edmondson, A. Mattevi, Structures of Human Monoamine Oxidase B Complexes with Selective Noncovalent Inhibitors: Saffinamide and Coumarin Analogs, *J. Med. Chem.* 50 (2007) 5848–5852, <https://doi.org/10.1021/jm070677y>.
- [40] N.M. O'Boyle, M. Banck, C.A. James, C. Morley, T. Vandermeersch, G. R. Hutchison, Open Babel: An open chemical toolbox, *J. Cheminform.* 3 (2011), <https://doi.org/10.1186/1758-2946-3-33>.
- [41] Q. Wu, Z. Peng, Y. Zhang, J. Yang, COACH-D: improved protein-ligand binding sites prediction with refined ligand-binding poses through molecular docking, *Nucleic Acids Res.* 46 (2018) W438–W442, <https://doi.org/10.1093/nar/gky439>.
- [42] S. Floris, A. Fais, A. Rosa, A. Piras, H. Marzouki, R. Medda, A.M. González-Paramás, A. Kumar, C. Santos-Buelga, B. Era, Phytochemical composition and the cholinesterase and xanthine oxidase inhibitory properties of seed extracts from the *Washingtonia filifera* palm fruit, *RSC Advances* 9 (2019) 21278–21287, <https://doi.org/10.1039/c9ra02928a>.
- [43] J. Yang, A. Roy, Y. Zhang, Protein-ligand binding site recognition using complementary binding-specific substructure comparison and sequence profile alignment, *Bioinformatics* 29 (2013) 2588–2595, <https://doi.org/10.1093/bioinformatics/btt447>.
- [44] O. Trott, A.J. Olson, AutoDock Vina: improving the speed and accuracy of docking with a new scoring function, efficient optimization, and multithreading, *J. Comput. Chem.* 31 (2010) 455–461, <https://doi.org/10.1002/jcc.21334>.
- [45] P. Pandey, N.D. Chaurasiya, B.L. Tekwani, R.J. Doerksen, Interactions of endocannabinoid virodhamine and related analogs with human monoamine oxidase-A and-B, *Biochem. Pharmacol.* 155 (2018) 82–91, <https://doi.org/10.1016/j.bcp.2018.06.024>.
- [46] G. Shipra, M. Gauri, P. Mohan Chandra, S. Prahlad Kishore, Identification of Novel Potent Inhibitors Against Bcl-xL Anti-apoptotic Protein Using Docking Studies, *Protein Peptide Lett.* 19 (2012) 1302–1317, <https://doi.org/10.2174/092986612803521602>.
- [47] S. Gupta, G. Misra, M.C. Pant, P.K. Seth, Prediction of a new surface binding pocket and evaluation of inhibitors against huntingtin interacting protein 14: an insight using docking studies, *J. Mol. Model.* 17 (2011) 3047–3056, <https://doi.org/10.1007/s00894-011-1005-8>.
- [48] U. Ammarah, A. Kumar, R. Pal, N.C. Bal, G. Misra, Identification of new inhibitors against human Great wall kinase using in silico approaches *Sci. Rep.* 8 (2018) 4894, <https://doi.org/10.1038/s41598-018-23246-0>.
- [49] R. Shalaby, J.P. Petzer, A. Petzer, U.M. Ashraf, E. Atari, F. Alasmari, S. Kumarasamy, Y. Sari, A. Khalil, SAR and molecular mechanism studies of monoamine oxidase inhibition by selected chalcone analogs, *J. Enzyme Inhib. Med. Chem.* 34 (2019) 863–876, <https://doi.org/10.1080/14756366.2019.1593158>.
- [50] E.M. Milczek, C. Binda, S. Rovida, A. Mattevi, D.E. Edmondson, The 'gating' residues Ile199 and Tyr326 in human monoamine oxidase B function in substrate and inhibitor recognition, *FEBS J.* 278 (2011) 4860–4869, <https://doi.org/10.1111/j.1742-4658.2011.08386.x>.
- [51] N. Chaurasiya, J. Zhao, P. Pandey, R. Doerksen, I. Muhammad, B. Tekwani, Selective Inhibition of Human Monoamine Oxidase B by Acacetin 7-Methyl Ether Isolated from *Turnera diffusa* (Damiana), *Molecules* 24 (2019) 810, <https://doi.org/10.3390/molecules24040810>.